JJMIE

Volume 15, Number 3, August. 2021
ISSN 1995-6665
Pages 291 - 300

Jordan Journal of Mechanical and Industrial Engineering

Effect of Gable Roof Angle on Natural Ventilation for an Isolated Building

Lip Kean Moey[a,*], Man Fai Kong[b], Vin Cent Tai[a], Tze Fong Go[c], Nor Mariah Adam[d]

[a]*Centre for Modelling and Simulation, Faculty of Engineering, Built Environment& Information Technology, SEGi University, Selangor, Malaysia*

[b]*Faculty of Engineering, Built Environment & Information Technology, SEGi University, Selangor, Malaysia*

[c]*Centre for Advance Materials and Intelligent Manufacturing, Faculty of Engineering, Built Environment & Information Technology, SEGi University, Selangor, Malaysia*

[d]*Department of Basic Science and Engineering, University Putra Malaysia Bintulu Sarawak Campus, Sarawak, Malaysia*

Received August 21 2020 *Accepted June 30 2021*

Abstract

Airflow characteristics around and within an isolated gable roof building were investigated using computational fluid dynamic with steady RANS equations. This study focuses on the following parameters: streamline of normalized velocity, pressure coefficient, and normalized turbulent kinetic energy. Three different roof pitches of the gable roof namely 15º, 25º, and 35º were considered. The streamline shows that an increase in roof pitch results in a corresponding increase of velocity at the window openings. Meanwhile, the streamline velocity at the roof opening varies across different roof angles. On the other hand, the pressure coefficient at the windward side and interior of the building decreases as the roof pitch becomes steeper. Variation in the flow fields of 25º and 35º roof pitch with window and roof opening, is relatively more apparent as compared to that of a 15º and 25º roof pitch. The turbulent kinetic energy at the leeward side of the building also becomes larger with the increase in roof pitch. Therefore, airflow behavior and characteristics are significantly dependent on the roof pitch which shows good agreement with the literatures. A higher roof pitch of gable roof building is, therefore, preferred for better ventilation rate.

Keywords: Natural Ventilation, Gable Roof, CFD, Roof Pitch, Steady RANS, Ventilation Rate;

1. Introduction

Malaysia as a tropical country is exposed to long-term solar heat attacks, global warming, and greenhouse effects. The Earth surface temperature has risen by 1°C over the past century[1], and is predicted to further rise over a range of 3.7°C to 4.8°C in the coming century[2]. In tropical countries, this rise of surface temperature has led to a sharp increase of energy consumption over the past decade. According to the Malaysian Energy Information Hub (MEIH), residential energy consumption has increased from 22.53-Terawatt hour (TWh) to a highest record of 31.16 TWh between the years of 2010 to 2017[3]. Renewable energy sources such as wind can offer important environmental, social and economic benefits[4,5].

Ventilation is a process that aids in improving indoor air quality and comfort by introducing cool and fresh air from a clean source into the building, while expelling existing hot and polluted air [6,7]. Ventilation also helps to optimize the indoor thermal environment, prevents excessive moisture development, and repels pollutants, such as pollens, dust, and contaminants in the air[8]. Excessive moisture build-ups especially in tropical countries may lead to allergies, respiratory diseases, besides the hygiene problems in environments that encourage molds and mites to thrive. Heat accumulation may also occur at roof and attic areas without the aid of ventilation. Thus, Heating, Ventilating and Air Conditioning (HVAC) systems are normally introduced to improve indoor air quality, comfort, and thermal environment. However, HVAC accounts up to 60% of domestic building energy consumption[7].

Natural ventilation utilizes natural phenomena such as wind force and the stack effect to introduce fresh air into an interior space and repel aged air to the outside. It is believed to be the most effective and environmentally friendly method of passive cooling for supply clean and fresh air to a space[8,9]. Natural ventilation with proper roof design is feasible for tropical countries such as Malaysia whereby local air conditions are classified as Class I, with annual wind velocities averaging between 1 m/s to 5 m/s[7]. Natural ventilation can be further categorized into cross ventilation and stack ventilation. Cross ventilation is driven by wind flow, thereby generating negative pressure indoors which in turn creates a pressure difference that directs the wind flow from outside into the building through apertures[7,10–12]. On the other hand, stack ventilation is driven by temperature discrepancies between the indoors and the outdoors of a building[8,13,14]. Due to the imperceptible indoor and outdoor temperature changes in tropical regions, cross ventilation is said to be more effective and therefore, the stack ventilation effect is not

* Corresponding author e-mail: moeylipkean@segi.edu.my.

included in the scope of this study[14]. Cross ventilation shall be the main focus of this investigation.

The roof plays an important role in preventing humidity development and heat accumulation in a building[15]. Roof configuration greatly impacts wind flow pattern and characteristics around and within a building and also controls the dispersion of pollutants[14–16]. Some common roof configurations in Malaysia are the hip, venturi, and gable types.

Computational Fluid Dynamics (CFD) is an authoritative tool that combines flow physics, computer application, mathematics, and the knowledge of mechanics to solve problems involving one or more phenomena such as fluid flow, heat change, mass transfer, and chemical reaction[17,18]. CFD was applied to study the airflow around a gable roof building with various roof tilt angles by measuring the turbulent kinetic energy, pressure coefficient, and time-averaged velocity around the gable roof building[19,20]. Reynolds-Averaged Navier-Stokes(RANS) models, such as the Standard k-ε (Sk-ε), Renormalization Group k-ε (RNG k-ε), Realizable k-ε (RK-ε), and Shear-Stress Transformation k-ω(SST k-ω) models were tested and validated against the wind tunnel experiment. These studies confirmed that roof pitches affect the streamline, distribution of turbulent kinetic energy, pressure coefficient, and mean velocity ratio of wind around the building.

Only a few literatures have comprehensively examined the impact of gable roof configuration on natural ventilation. Karava et al. analyzed the wind-induced natural ventilation on a 1:12 sloped gable roof building using the boundary layer wind tunnel experiment[6]. The tested building model has a 153mm × 98mm rectangular plan view with 30mm in eave height. This experiment was conducted on a gable roof building with windward wall porosity ranging from 0 to 22%. Results indicate that the internal pressure coefficient and discharge coefficient of a cross-ventilated building varies significantly with wall porosity and inlet to outlet ratio. Non-uniformity of the internal pressure coefficient for windward wall porosity larger than 10% was only observed in a cross-ventilated building. The airflow rates changed considerably when different discharge coefficients are used, specifically for configurations with large inlet to outlet ratios.

Peren et al. investigated the impact of roof angle and opening locations on cross ventilation of a generic isolated building with asymmetric opening positions[21]. The analysis was conducted with 3D RANS CFD simulation using six turbulence models and five different roof angle inclinations. Accuracy of the SST k-ω model was validated against the Particle Image Velocimetry (PIV) experiment by Karava et al.[22]. Results indicate that the volume flow rate and indoor air flow pattern are highly dependent on the roof inclination angles. Critical roof inclination angle shall be larger than 18º to improve the volume flow rate of a low-rise building.

In reality, volume flow rate, pressure difference over a building, and indoor air speed rely strongly on roof shapes and configurations[22]. However, limited literatures focus on the effect of roof configuration on indoor natural ventilation. As such, the impact of a gable roof building on indoor airflow pattern has yet to be well studied specifically in buildings with window openings. Therefore, this study is dedicated to investigate the effect of gable roof angles on natural cross ventilation in an isolated building with window openings. The CFD simulation results generated are then validated against experimental and numerical analysis performed by Karava et al.[22]and Tominaga et al.[23],respectively.

The remaining of the paper is organized as follows: Section 2 outlines the computational setting and parameters, perform model validation, and grid sensitivity studies. Section 3 presents the simulation results of gableroof building with various roof pitches and discusses the effect of varied gable roof angles on airflow characteristics. Finally, section 4 concludes the findings of this study.

2. Numerical Studies: Model Setup and CFD Simulation

2.1. Model Cases

In this study, an isolated basic building model is chosen as the reference model. The model has a 1:50 scaled down dimension of length × width × height (L×W×H) = 100mm × 100mm × 80mm, correspondingto 5m × 5m × 4m in real scale. This model also constitutes of a set of window and roof openings each at two opposing side walls, having heights of 18 mm and 9 mm respectively with center line of the window opening at y = 0.04 m, and that of the roof opening at y=0.0655 m from ground level. Wall thickness of the tested model is 2 mm as proposed by Ramponi et al.[14]. This basic model was used as a basis for grid sensitivity study in which its results were validated by the PIV experiment by Karava et al.[22].Three model cases were constructed based on this basic building model using different roof pitches. Another reference model with a gable roof but without window openings was also created with reference to Tominaga et al.[23]for validation purposes.

2.2. Computational Domain and Grids

Simulations were performed using a scaled down model which was modified based on the basic building model. The computational domain was created with reference to existing recommendedoperational guidelines proposed by Franke et al.[24]and Tominaga et al.[25]. However, distance between the inlet plane of the computational domain and windward wall of the testedmodel was reduced to 3H at upstream instead of 5H as recommended by Franke et al.[24]and Tominaga et al.[25] to restrict the extent of unplanned streamwise gradient[14]. The top and lateral wall of the flow domain were set 5H away from the model, while the downstream length was set to 15H. Figures1(a) and 1(b) illustrate the dimensions of a gable roof building with roof angle of 15º and the computational domain, respectively, whereby H is the effective building height measured from ground level.

Mosaic^{TM} meshing technology was applied to this geometry due to its ability to produce high quality octree hexahedron in the bulk region. The Mosaic^{TM} meshing technology allows automatic connection of elements regardless of their types. It also produces high quality meshes and is efficient in solving fluid flow around highly complex geometries[26]. This geometry was first meshed with a tetrahedral element using the scope sizing function in

Ansys Fluent, followed by its conversion into a poly-hexcore. Figure 2 shows the meshing details of the tested models and the flow domain.

2.3. Boundary Conditions

The measured mean wind speed and turbulence intensity from the vertical plan determines the boundary conditions to be imposed at the inlet plane of the flow domain. Inlet wind velocity was determined using equation (1), whereby z_0=0.00003m, von Karman constant $\kappa = 0.42$, z is the height coordinate, and U_{abl} is friction velocity of the atmospheric boundary layer. Turbulent kinetic energy (TKE), k can then be calculated using equation (2), knowing the mean wind velocity and measured turbulence intensity, I_u. The chosen α value shall be 1 as recommended by Tominaga et al.[23].The turbulence dissipation rate, ε and specific dissipation rate, ω can be determined using equations (3) and (4) respectively whereby $C_\mu$is an empirical constant equal to 0.09 [27].

$$U(z) = \frac{u^*_{ABL}}{\kappa}\ln(\frac{z+z_0}{z}) \quad (1)$$

$$k(z) = \alpha\left(I_u(z)U(z)\right)^2 \quad (2)$$

$$\varepsilon(z) = (\frac{u^{*3}_{ABL}}{\kappa(z+z_0)}) \quad (3)$$

$$\omega(z) = \frac{\varepsilon(z)}{C_\mu k(z)} \quad (4)$$

Standard wall function with roughness height modification was applied at ground surface[28,29] as this building is expected to be built on a grass covered terrain with a scaled down roughness length of 0.00003m. The sand grain roughness k_s was determined using equation (5) derived by Blocken et al.[30]which describes the consistency of relationship between k_s and the roughness constant C_s, whereby the chosen value for C_s is 0.42.

$$k_s = \frac{9.793z_0}{C_s} \quad (5)$$

Zero static pressure was imposed at the outlet plane, and symmetry type was applied to the symmetry plane. Boundary condition at the top and lateral side wall of the flow domain on the other hand were imposed with zero normal gradients and velocities representing the zero-shear condition. Standard wall function with zero roughness height was also applied to the tested model.

2.4. Solver Settings

In this study, simulations were performed using Ansys 2019 R3. The 3D steady RANS equation was solved by theSST k-ω turbulence model. The SST k-ω model was selected as it has better accuracy in comparison to the PIV experiment conducted by Karava et al.[22]. This study also uses the SIMPLE algorithm which was established from the Green Gauss node based spatial discretization in combination with second-order upwind discretization schemes and pressure interpolation applied to the convection and viscous terms of the governing equation. Convergence was expected to be achieved when the scaled residuals are receding down to 10^{-4}. Table 1 summarizes the details and comparison of parameters between previous literatures.

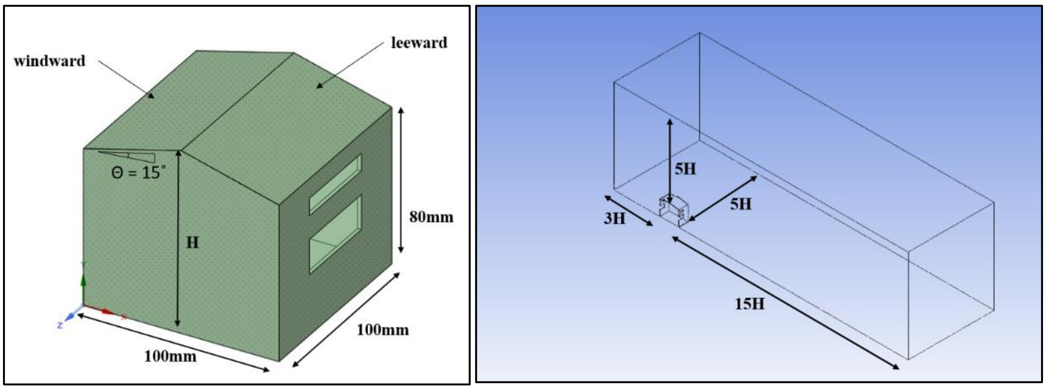

(a) (b)

Figure 1. Dimension of (a)15˚ gableroof building and (b) computational domain

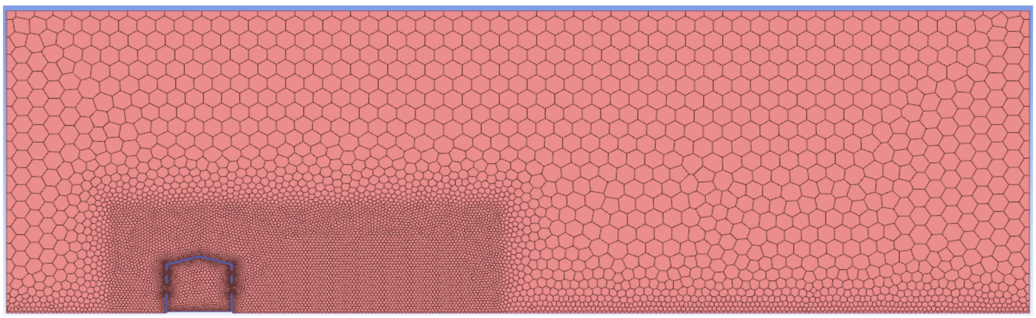

Figure 2. Meshing details of flow domain of 15º roof pitch

2.5. Grid Sensitivity Analysis

A grid sensitivity analysis was performed on the basic building model to ensure that the results are grid independent. Three different grids with various cell counts (319426, 473837 and 749997) were created for the purpose of this analysis.Grids with higher cell counts have smaller mesh sizes. Results of these meshes were compared with the PIV results by Karava et al.[22] in terms of dimensionless mean velocity ratio (U/U_{ref}) across the inlet and outlet aperture. Note that U is the 3D streamwise velocity vector and U_{ref} = 6.97m/s is the reference wind speed measured at the building height (H=80mm).

Figure 3 illustrates the results obtained from three different grid sizing and the PIV results by Karava et al. [22]. Each coarse, basic and fine mesh (denoted by grid A, B and C) has respective cell counts of 319426, 473837, and 749997. Results were compared in terms of dimensionless mean velocity ratio U/U_{ref}. Observations clearly show that the fine mesh model conforms most closely to the experimental results with the nearest cell counts as compared to the literatures in Table 1. The fine mesh is, therefore, implemented in the subsequent simulations and studies. To effectively capture the boundary layer around the building walls, 10 prism layers with the 1st cell height of 0.01mm (corresponding to $y^+ \approx 200$) and an inflation rate of 1.2 were added to the mesh. Noticeable difference between the numerical and experimental results can be observed near the openings. This is attributed to the fact that numerical models tend to overestimate the mean wind speed near the openings[10]. Also, shading effects and reflections may contribute to inaccurate prediction of the PIV measurements[6].

2.6. Model Validation

Both the wind-tunnel experiment and CFD simulation conducted by Tominaga et al.[23]were used for model validation. The test model was created without any window and roof opening for this validation purpose. Mean velocity ratio around the simulated models were then compared to that of the wind tunnel measurements and computational results by Tominaga et al.[23].

The model was validated with respect to the reference model by Tominaga et al. [23] in terms of streamlines and pressure coefficient. Figures 4 and 5 compare the streamline and distribution of pressure coefficient between the validation model and that of the reference model. Results show a large recirculation region behind the building and a small recirculation region at the lower corner windward side of the building. Positive pressure is also observed in front of the validation model due to the blockage caused by the building structure. Negative peaks at the front corner of the validation model were also apparent in both results. Further detailed inspection of Figure 4 revealed a wake behind the validation model that is larger than that of the reference model. This is because the$k-\omega$ SST turbulence model was used for validation while the RNG $k-\varepsilon$ model was used as reference. Both RANS models perform differently in turbulence prediction[23]. Although significant improvement on prediction accuracy can be achieved by systematically optimizing the closure coefficients of the RANS models[32], the work is beyond the scope of this study. This validation model is therefore practiced and modified accordingly in the following investigations.

Table 1. Summary of literature reviews on roof configurations

Literature	Roof Shape	Roof Pitches (°)	Turbulence Model	Mesh Type	Selected Cell Counts
Tominaga et al.,2015[23]	Gable	16.7, 26.6, 36.9	Sk-ε, RNG k-ε, Rk-ε, SST k-ω	Structured	2355280
Ozmen et al., 2016 [31]	Gable	15, 30, 45	Rk-ε, Sk-ω	Structured	800000
Peren et al., 2015[21]	Inclination	9, 18, 27, 36, 45	SST k-ω	Structured	770540
Karava et al., 2007[6]	Gable	5	-	-	-

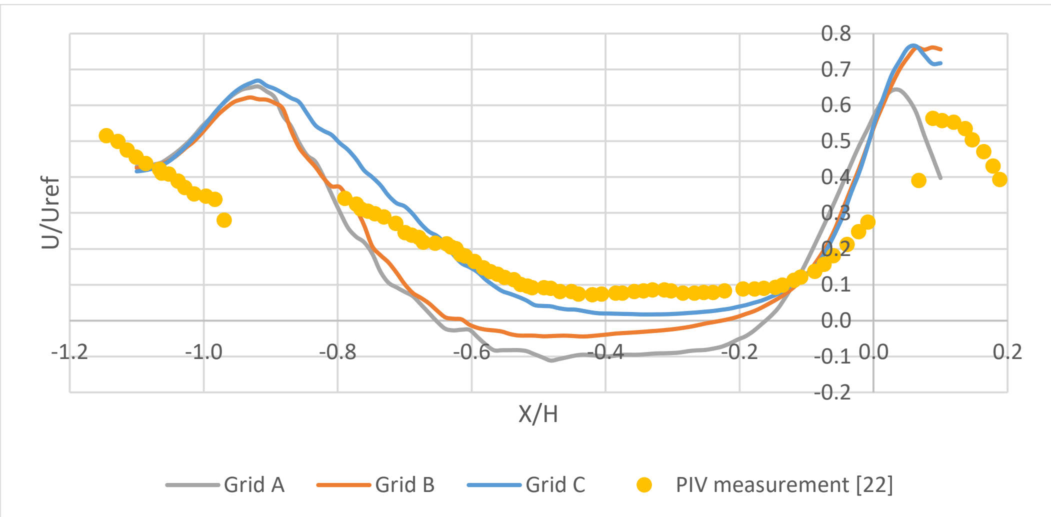

Figure 3. Comparison between simulation results of three different grid sizing and PIV experimental results by Karava et al. [22]

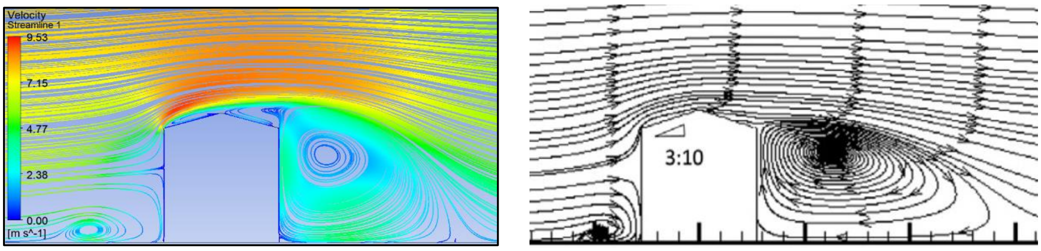

(a) (b)

Figure 4. Comparison of streamline velocity between (a) validation model of 15º roof pitch and (b) reference model of 16.6º [23].

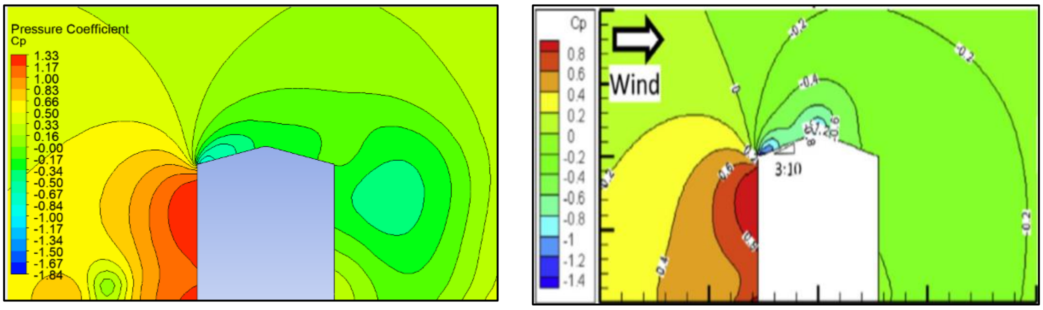

(a) (b)

Figure 5. Comparison of pressure coefficient contour of (a) validation model of 15º roof pitch and (b) reference model [23].

3. Results and Discussion

3.1. Streamlines

Figure 6 compares the streamlines of normalized velocity for various roof pitches. According to Tominaga et al.[23], the recirculation region at the leeward side of the building becomes larger as roof angle increases. The center region of the recirculation eddy behind the building also tends to move upwards. However, addition of window and roof openings, and shelling of the model allowed wind to flow through the building thereby interrupting the recirculation flow behind the model. It can be clearly observed that there is a noticeable change in flow field between roof pitches of 15º and 25º. Although no reverse flow is observed behind the building for roof pitch of 15˚, but reverse flow is present, and it becomes larger in roof pitches of 25º and 35º. Velocity through the openings are also observed to be increasing as the roof angle becomes steeper. The resulting critical roof pitch is nearly compatible with the critical roof pitch of 18º at which flow around the gable roof building changes, and the reversed flow at the leeward side of the roof becomes larger. Overall streamline results are in well agreement with the findings by Tominaga et al.[23].

3.2. Spatial Distribution of Pressure Coefficient

Figure 7 presents a comparison of the static pressure around a building with various gable roof angles. In all cases, peak positive value of pressure coefficient is observed at the front of the building due to the impact of wind force on the building wall. Negative peak value on the other hand is observed at the windward corner and the ridge side in the case of a 15º gable roof. Pressure coefficient also increases with increment in roof angle at the windward side. Contrastingly, no negative peak value of pressure coefficient is observed at the windward corner of the 25º and 35º roof pitches. However, the negative value nearing the leeward side of the roof becomes larger as the steepness of the roof pitch increases , and the wake formation region becomes larger with increment in the roof angle. Pressure within the building also decreases with an increase in the roof pitch.

3.3. Mean Velocity Profile

Figure 8 shows the inlet and outlet profiles of dimensionless streamwise mean velocity, U/Uref at the windward window and roof openings (RO) of the tested model. Results clearly indicate that velocity at both window and roof openings increased with increasing roof pitch. A notable difference is observed between roof pitches of 25º and 35º. Constant changes are also observed in the streamwise mean velocity profile at the roof opening inlet when roof pitch is increased. Similarly, significant difference in velocity profile is observed at the window outlet between all three roof pitches whereby a prominent increase is observed between the 15º and 25º roof pitch, followed by an abrupt decrease in the case of the 35º roof pitch. The velocity profile has also changed noticeably. Results, therefore, indicate that dimensionless streamwise mean velocity is strongly dependant on the roof pitch.

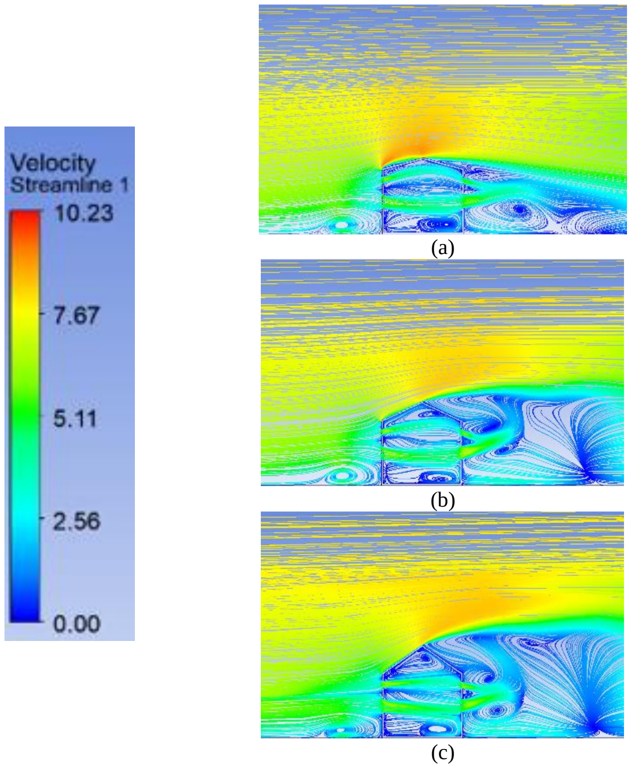

Figure 6. Streamlines of Normalized Velocity (U/Uref) of (a)15˚ roof pitch, (b)25˚ roof pitch and (c)35˚ roof pitches

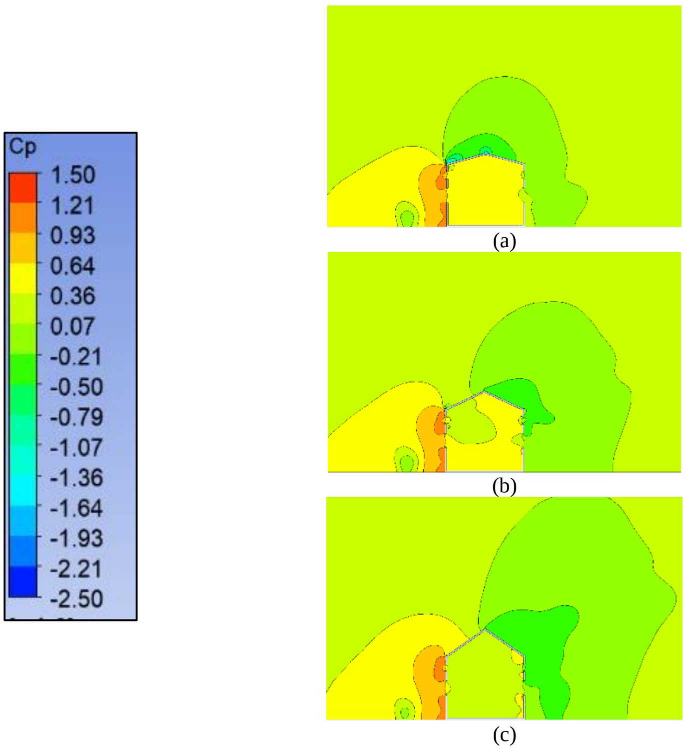

Figure 7. Spatial distribution of pressure coefficient of (a)15˚, (b)25˚ and (c)35˚ roof pitches

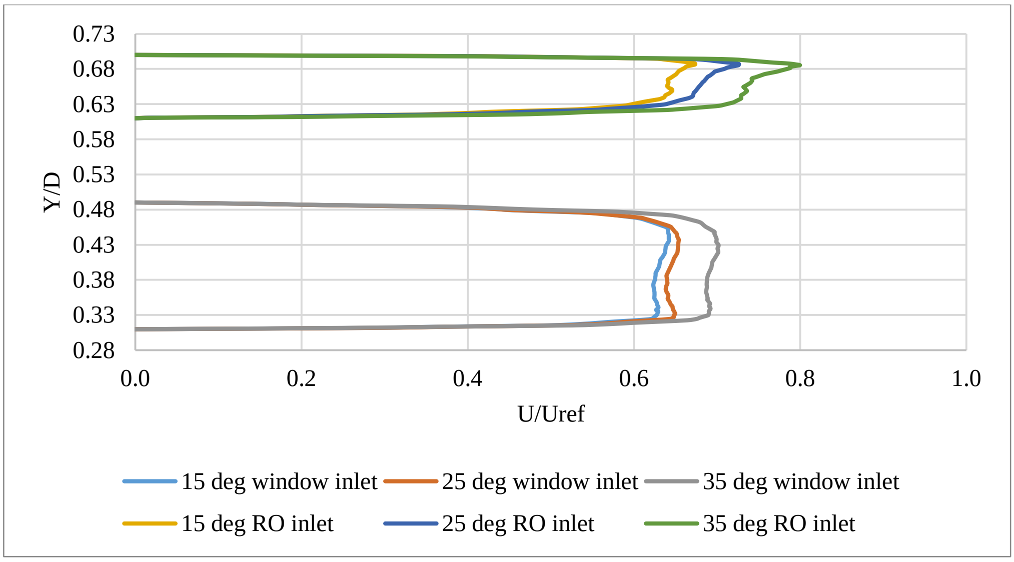

(a)

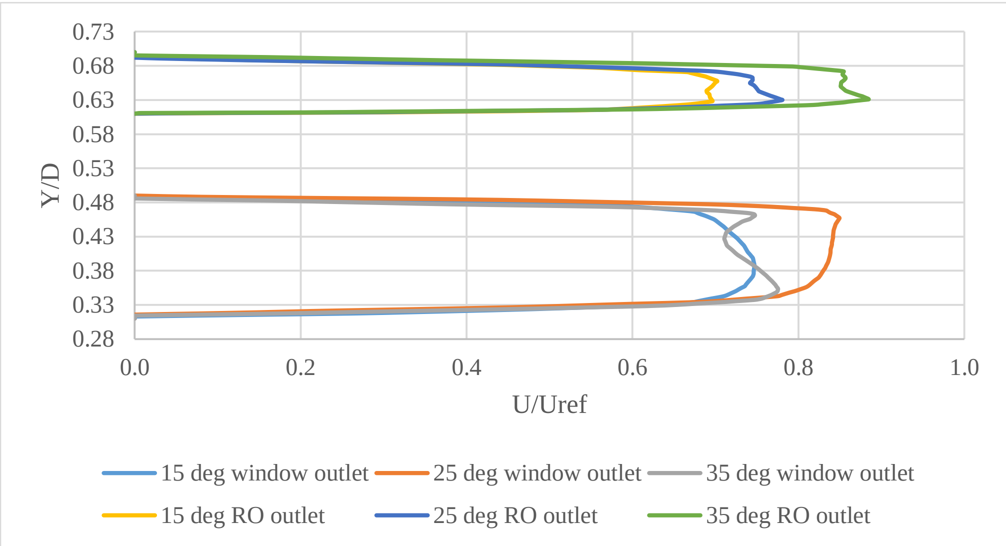

(b)

Figure 8. Velocity profile at window and roof opening (a) inlet and (b) outlet

3.4. Distributions of Normalized Turbulent Kinetic Energy

Figure 9 illustrates the distribution contours of normalized turbulent kinetic energy (TKE), k for 15º,25º and 35º roof pitches. In the case of a 15º roof pitch, region of distribution of TKE is observed to be small with no apparent peak value. However, the peak value of TKE is observed at the ridge in the case of 25º and 35º roof angles, with both peak value and region of TKE distribution becoming larger as the roof pitch becomes steeper. This is due to flow separation resulting from the increment in roof angle[23]. In contrast, changes in the distribution of TKE is minor within the building despite changes in the roof angle. The TKE distribution near the roof opening outlet on the other hand was observed to be larger as the roof pitch increased. This TKE distribution shows the airflow power near the building from ambient wind through the apertures, therefore accounting for the flow patterns near the building model which explains the sudden change of streamwise mean velocity profile at the window outlet for roof pitch of 35º[33].

3.5. Ventilation Rate

The air flow rate of a naturally ventilated building model can usually be determined by means of simple relationship. The rate of ventilation for a naturally cross ventilated low rise isolated building can be determined using the following equations[34]:

$$C_p = \frac{P - P_r}{\frac{1}{2}\rho V_{ref}^2} \quad (6)$$

$$CQ = C_a V_{ref} \sqrt{\Delta C_P} \quad (7)$$

$$C_a = \frac{CQ}{(1 + CQ)} \quad (8)$$

$$Q = C_a V_{ref} A_e \quad (9)$$

Equation (6) is used to determine the pressure coefficient, C_P, whereby P is the pressure at selected opening, P_r is the reference free stream static pressure, $\rho = 1.225 kg/m^3$ is the density of air, and $V_{ref} = 6.97$ m/s is the measured velocity at reference height. The pressure coefficient calculated from inlet and outlet openings will then be used in equation (7) to calculate the estimated flow coefficient, C_Q, whereby $C_d = 0.62$ is the discharge coefficient and ΔC_P is the pressure coefficient change between inlet and outlet opening. Accordingly, ventilation rate can be calculated by equation (9) which is derived from the Bernoulli equation namely the product of actual flow coefficient: C_a, V_{ref}, and the effecitve area of opening: A_e. In this present study, the effective area (A_e) was determined to be 1.242 x $10^{-3}m^2$, whereby the corresponding discharge coefficient can be reasonably assumed to be 0.62 - a typical value for a sharp openings.

Figure 10 compares the ventilation rates between the three different roof pitches. Data clearly indicate that ventilation rate increases with the increase in roof pitch. A larger difference is observed in the ventilation rate between 15º and 25º roof angle and the increment of ventilation ratedecedes when the roof angle increased to 35º from 1.97% to 0.69%. This is caused by the pressure difference between the interior and exterior of the building model. The pressure variation between indoors and outdoors causes the wind flow to enter the building at an increasing velocity through the opening apertures. This increment of wind speed entering the building with increasing roof pitch induces a higher rate of ventilation and eventually promotes improved indoor air quality and comfort.

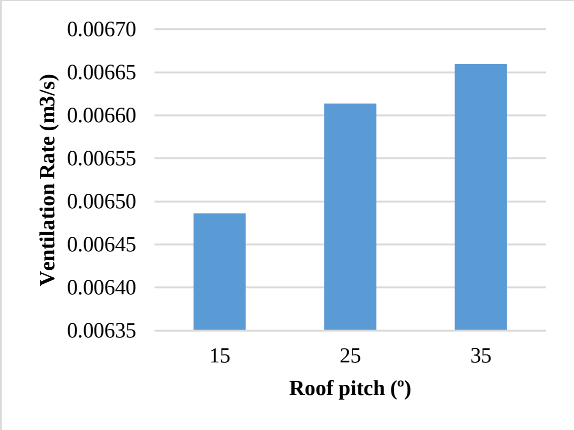

Figure 10. Comparison of ventilation rate (m^3/s) of gable roof with various angle.

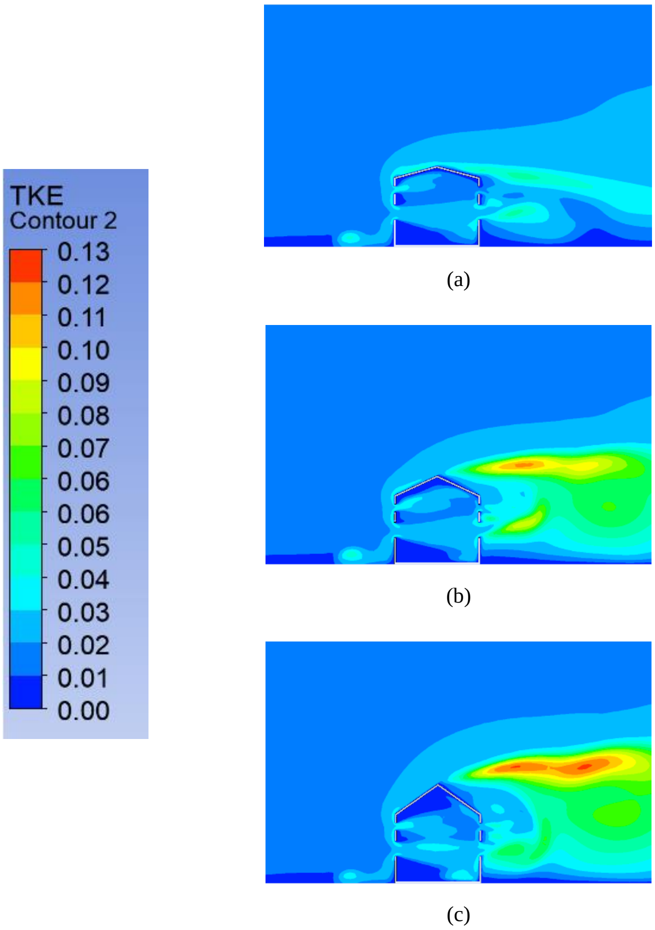

Figure 9. Distribution of normalized turbulent kinetic energy of (a)15˚, (b)25˚ and (c)35˚ roof pitch

4. Conclusion

In the present study, airflow characteristics around and within an isolated building with gable roof of varied roof angles namely 15º, 25º, and 35º were investigated and analyzed by the means of computational analysis and 3D RANS in steady state. Model validation was conducted and verified to be agreeable with the findings from literature. Computational simulation results also show that the streamline, pressure coefficient, TKE, mean velocity ratio, and ventilation rate are significantly dependent on the roof pitch. The recirculation region behind the building tends to move upwards and become larger with the increase in roof pitch angle. However, the presence of window and roof openings generates wind flow through the apertures thereby disturbing the recirculation region. Positive pressure was observed at the windward side of the building due to the wind blockage caused by the building wall. Negative peaks on the other hand occur at the windward corner and reduces until it eventually diminishes as the roof pitch is increased. Concurrently, the spatial distribution of TKE at the leeward side of the building roof becomes larger as the roof pitch is increased. Ventilation rate was also observed to increase with higher roof pitch. Based on all the above measured parameters, it can be concluded that gable roofs with a higher roof pitch is preferred for better natural ventilation in an isolated building. This study is, however, limited only to one reference wind speed:U_{ref} = 6.97m/s, and one wind direction namely that perpendicular to the windward side of the building. As ventilation performance could be affected by varying the reference wind speed and wind direction, these parameters may be further investigated in future research. Future work can also include the surrounding buildings to better understand the effect of real urban conditions on cross ventilation.

References

1. A.P. Aizebeokhai, "Global warming and climate change: Realities, uncertainties and measures". International Journal of Physical Sciences, Vol. 4, No.13, 2009, 868–879.
2. N.A. Hassan, Z. Hashim, J.H. Hashim, "Impact of climate change on air quality and public health in urban areas". Asia-Pacific Journal of Public Health, Vol. 28, No. 2, 2014, 38–48.
3. Suruhanjaya Tenaga. Malaysia energy statistics handbook 2019. Malaysia Suruhanjaya Tenaga (Energy Comm); 2019, p.1–86.
4. S. A. Ahmed, H. O. Mahammed, "A statistical analysis of wind power density based on the weibull and ralyeigh models of “Penjwen region” Sulaimani/Iraq". Jordan Journal of Mechanical and Industrial Engineering, Vol. 6, No. 2, 2012, 135-140.
5. H. Nidal, "Greenhouse gas emissions reduction potential of Jordan’s utility scale wind and solar projects". Jordan Journal of Mechanical and Industrial Engineering, Vol. 10, No. 3, 2016, 199-203.
6. P. Karava, T. Stathopoulos, A.K. Athienitis, "Wind-induced natural ventilation analysis". Solar Energy, Vol. 81, No. 1, 2007, 20–30.
7. L.K. Moey, N.M. Adam, K.A. Ahmad, L.C. Abdullah, "Wind tunnel study of different roof geometry configurations for wind induced natural ventilation into stairwell in tropical climate". International Journal of Engineering Research, Vol. 13, No.5, 2018, 2635–47.
8. C.H. Lim, S. Omidreza, K. Sopian, M.Y. Sulaiman, S. Mat, E. Salleh, "Design configurations analysis of wind-induced natural ventilation tower in hot humid climate using computational fluid dynamics". International Journal of Low-Carbon Technologies, Vol. 10, No. 4, 2013, 332–346.
9. M. N. Khan, I. Janajreh, "Transevaporative cooling performance of a three-sided wind catcher". Jordan Journal of Mechanical and Industrial Engineering, Vol. 11, No. 4, 2017, 225-233.
10. R. Ramponi, B. Blocken, "CFD simulation of cross ventilation flow for different isolated building configurations:Validation with wind tunnel measurements and analysis of physical and numerical diffusion effects". Journal of Wind Engineering and Industrial Aerodynamics, Vol. 104-106, 2012, 408-418.
11. M. Shirzadi, P.A. Mirzaei, M. Naghashzadegan, "Development of an adaptive discharge coefficient to improve the accuracy of cross-ventilation airflow calculation in building energy simulation tools". Building and Environment, Vol.127, 2018, 277–290.
12. M. Shirzadi, M. Naghashzadegan, P.A. Mirzaei, "Improving the CFD modelling of cross-ventilation in highly-packed urban areas". Sustainable Cities and Society, Vol.37, No.Sieminski 2015, 2018, 451–65.
13. A. Aflaki, N. MahyuddinN, Z.A. Mahmoud, B. Mohamad Rizal, "A review on natural ventilation applications through building façade". Energy and Buildings, Vol.101, 2015, 153-162.
14. R. Ramponi, B. Blocken, "CFD simulation of cross-ventilation for a generic isolated building: Impact of computational parameters". Building and Environment,Vol. 53, 2012, 34–48.
15. J. Kindangen, G. KraussG, P. Depecker, "Effects of roof shapes on wind-induced air motion inside buildings". Building and Environment, Vol.32, No.1, 1997, 1–11.
16. L. K. Moey, N. M. Adam, K. A. Ahmad, "Effect of venturi-shaped roof angle on air change rate of a stairwell in tropical climate". Journal of Mechanical Engineering, Vol. 4, No. 4, 2017, 135-150.
17. Y. Huang, X. Hu, N. Zeng, "Impact of wedge-shaped roofs on airflow and pollutant dispersion inside urban street canyons". Building and Environment, Vol. 44, No.12, 2009, 2335–2347.
18. M.F. Yassin, "Impact of height and shape of building roof on air quality in urban street canyons". Atmospheric Environment, Vol. 45, No. 29, 2011, 5220–5229.
19. Y. Tominaga, B. Blocken, "Wind tunnel experiments on cross-ventilation flow of a generic building with contaminant dispersion in unsheltered and sheltered conditions". Building and Environment, Vol.92, 2015, 452–461.
20. R.K. Raman, Y. Dewang, J. Raghuwanshi, "A review on applications of computational fluid dynamics". International Journal of Laskshmi Narain College of Technology, Vol. 2, No. 6, 2018, 137–143.
21. J.I. Perén, T. vanHooff, B.C.C. Leite, B. Blocken, "CFD analysis of cross-ventilation of a generic isolated building with asymmetric opening positions: Impact of roof angle and opening location". Building and Environment, Vol. 85, 2015, 263–276.
22. P. Karava, T. Stathopoulos, A.K. Athienitis, "Airflow assessment in cross-ventilated buildings with operable façade elements". Building and Environment, Vol. 46, No.1, 2011, 266–279.
23. Y. Tominaga, S. Akabayashi, T. Kitahara, Y.Arinami, "Air flow around isolated gable-roof buildings with different roof pitches: Wind tunnel experiments and CFD simulations". Building and Environment,Vol. 84, 2015, 204–213.
24. Franke J, Hellsten A, Schlunzen H, Carissimo B. Best practice guideline for the CFD simulation of flows in the urban environment. 1st ed. Belgium: COST Action; 2007, p. 10–26

25. Y. Tominaga, A. Mochida, R. Yoshie, H. Kataoka, T. Nozu, M. Yoshikawa, "AIJ guidelines for practical applications of CFD to pedestrian wind environment around buildings". Journal of Wind Engineering and Industrial Aerodynamics, Vol. 96, 2008, 1749–1761.
26. Z. Krishna, P. Gandhar, S. Balasubramanyam, A. Varghese, "Ansys mosaic poly-hexcore mesh for high-lift aircraft configuration". 21 st Annual CFD Symposium, Bangalore, India, 2019,1–11.
27. M. Shirzadi, P.A. Mirzaei, M. Naghashzadegan, Y. Tominaga, "Modelling enhancement of cross-ventilation in sheltered buildings using stochastic optimization". International Journal of Heat and Mass Transfer, Vol. 118, 2018, 758–772.
28. Cebeci T, Bradshaw P. Momentum transfer in boundary layers. New York: Hemisphere Publishing Corporation; 1977, 377–386.
29. B.E. Launder, D.B. Spalding, "The numerical computation of turbulent flows". Computer Methods in Applied Mechanics and Engineering, Vol. 3, No. 2, 1974, 269–289.
30. B. Blocken, T. Stathopoulos, J. Carmeliet, "CFD simulation of the atmospheric boundary layer: Wall function problems". Atmospheric Environment, Vol. 41, No. 2, 2007, 238-252.
31. Y. Ozmen, E. Baydar, J.P.A.J. vanBeeck, "Wind flow over the low-rise building models with gabled roofs having different pitch angles". Building and Environment, Vol.95, 2016, 63–74.
32. M. Shirzadi, P.A. Mirzaei, M. Naghashzadegan, "Improvement of k-epsilon turbulence model for CFD simulation of atmospheric boundary layer around a high-rise building using stochastic optimization and Monte Carlo Sampling technique". Journal of Wind Engineering and Industrial Aerodynamics, Vol.171, No.October, 2017, 366–379. No.October:366–79.
33. S. Hawendi, S. Gao, "Impact of windward inlet-opening positions on fluctuation characteristics of wind-driven natural cross ventilation in an isolated house using LES". International Journal of Ventilation, Vol. 17, No. 2, 2018, 93–119.
34. M. Swami, & S. Chandra, "Procedures for calculating natural ventilation airflow rates in buildings". ASHRAE Final Report, Cape Canaveral, Florida, FSEC-CR-163-86, 1987.